

# Nano-opto-mechanical actuator driven by gradient optical force

Cai, H.; Xu, K. J.; Liu, A. Q.; Fang, Q.; Yu, M. B.; Lo, Guo-Qing.; Kwong, Dim Lee.

2012

Cai, H., Xu, K. J., Liu, A. Q., Fang, Q., Yu, M. B., Lo, G. Q., et al. (2012). Nano-opto-mechanical actuator driven by gradient optical force. *Applied Physics Letters*, 100(1).

<https://hdl.handle.net/10356/95290>

<https://doi.org/10.1063/1.3673854>

---

© 2012 American Institute of Physics. This paper was published in *Applied Physics Letters* and is made available as an electronic reprint (preprint) with permission of American Institute of Physics. The paper can be found at the following official DOI: [<http://dx.doi.org/10.1063/1.3673854>]. One print or electronic copy may be made for personal use only. Systematic or multiple reproduction, distribution to multiple locations via electronic or other means, duplication of any material in this paper for a fee or for commercial purposes, or modification of the content of the paper is prohibited and is subject to penalties under law.

*Downloaded on 23 Aug 2022 13:10:13 SGT*

## Nano-opto-mechanical actuator driven by gradient optical force

H. Cai, K. J. Xu, A. Q. Liu, Q. Fang, M. B. Yu et al.

Citation: *Appl. Phys. Lett.* **100**, 013108 (2012); doi: 10.1063/1.3673854

View online: <http://dx.doi.org/10.1063/1.3673854>

View Table of Contents: <http://apl.aip.org/resource/1/APPLAB/v100/i1>

Published by the [American Institute of Physics](#).

### Related Articles

Experimental characterisation of a novel viscoelastic rectifier design  
*Biomechanics* **6**, 044112 (2012)

Focused ion beam milling and deposition techniques in validation of mass change value and position determination method for micro and nanomechanical sensors  
*J. Appl. Phys.* **112**, 114509 (2012)

Analyzing threshold pressure limitations in microfluidic transistors for self-regulated microfluidic circuits  
*Appl. Phys. Lett.* **101**, 234107 (2012)

Note: Helical nanobelt force sensors  
*Rev. Sci. Instrum.* **83**, 126102 (2012)

Integrating magnetoresistive sensors with microelectromechanical systems for noise reduction  
*Appl. Phys. Lett.* **101**, 234101 (2012)

### Additional information on *Appl. Phys. Lett.*

Journal Homepage: <http://apl.aip.org/>

Journal Information: [http://apl.aip.org/about/about\\_the\\_journal](http://apl.aip.org/about/about_the_journal)

Top downloads: [http://apl.aip.org/features/most\\_downloaded](http://apl.aip.org/features/most_downloaded)

Information for Authors: <http://apl.aip.org/authors>

## ADVERTISEMENT

**AIP** | Applied Physics  
Letters

**SURFACES AND INTERFACES**  
Focusing on physical, chemical, biological, structural, optical, magnetic and electrical properties of surfaces and interfaces, and more...

**ENERGY CONVERSION AND STORAGE**  
Focusing on all aspects of static and dynamic energy conversion, energy storage, photovoltaics, solar fuels, batteries, capacitors, thermoelectrics, and more...

**EXPLORE WHAT'S NEW IN APL**

**SUBMIT YOUR PAPER NOW!**

## Nano-opto-mechanical actuator driven by gradient optical force

H. Cai,<sup>1,a)</sup> K. J. Xu,<sup>2</sup> A. Q. Liu,<sup>2</sup> Q. Fang,<sup>1,3</sup> M. B. Yu,<sup>1</sup> G. Q. Lo,<sup>1</sup> and D. L. Kwong<sup>1</sup>

<sup>1</sup>*Institute of Microelectronics, A\*STAR (Agency for Science, Technology and Research),  
11 Science Park Road, Science Park II, Singapore 117685*

<sup>2</sup>*School of Electrical & Electronic Engineering, Nanyang Technological University, 50 Nanyang Avenue,  
Singapore 639798*

<sup>3</sup>*Optoelectronic System Laboratory, Institute of Semiconductors, Chinese Academy of Sciences,  
Beijing 100083, China*

(Received 7 August 2011; accepted 10 December 2011; published online 5 January 2012)

In this letter, a nanoscale opto-mechanical actuator driven by gradient optical force is designed and demonstrated. The nanoscale actuator can achieve a maximum displacement of 67 nm with a response time of 94.5 ns. The optical force is estimated as 1.01 pN/ $\mu\text{m}/\text{mW}$  in C-band operating wavelengths. The device is fabricated on silicon-on-insulator wafer using standard dry etching processes. Compared with traditional microelectromechanical systems actuators driven by electrostatic force, the nanoscale opto-mechanical actuator has the advantages of high resolution of actuation, nanoscale displacement, and fast operating speed. It has potential applications in optical signal processing, chemical, and biological sensing. © 2012 American Institute of Physics. [doi:10.1063/1.3673854]

Silicon-based microelectromechanical systems (MEMS) actuators driven by electrostatic force are widely used for microscale actuating applications, such as switches,<sup>1,2</sup> interferometers,<sup>3</sup> and tunable lasers.<sup>4</sup> However, there are limitations in terms of nanoscale displacement control, resolution, tuning speed, pull-in instability, etc.<sup>5–7</sup> Meanwhile, in those electrostatic MEMS actuator (e.g., parallel plate-plate and comb-drive actuators), the magnitude of the capacitance-dependent electrostatic force is determined by the plate area, which is in the scale of micrometers. When the dimension of the plate is scaled down from micrometers to nanometers, the plate overlapping area has to be reduced accordingly, resulting in insufficient electrostatic force to drive the actuator. Furthermore, the electronic and mechanical-thermal noise may degrade the performance of the electrostatic force. Therefore, it is difficult to design a nanoscale actuator based on the conventional concept of the capacitance-dependent electrostatic force.

Optical force has recently attracted significant interests, especially in the areas of nanoparticle trapping and manipulation<sup>8–10</sup> and optomechanically driven nanostructures.<sup>11–14</sup> Transverse gradient force, which is one of the optical force, acts transversely to the light propagation direction and can be increased by the orders of magnitude in evanescently coupled waveguides due to the largely enhanced gradient in the near field of guided wave structures.<sup>15</sup> It was recently proposed that the enhanced gradient optical force may result in submicrometer and nanometer displacements using milliwatt input power.<sup>16</sup> It has also been demonstrated in nanophotonic waveguide to produce mechanical displacement of integrated nanophotonic structures.<sup>15–17</sup> Different from the dimension-dependent electrostatic force, the gradient optical force is power-dependent force, which is beyond dimension limitations. Hence, optical force based nanoscale

actuator has a different design concept from traditional silicon-based MEMS actuator.

In this letter, a nanoscale optomechanical actuator driven by gradient optical force is designed, fabricated, and demonstrated. It consists of a nanoscale free-hanging waveguide, a parallel bus waveguide, a shutter and two fold-beams with supporting anchors as shown in Fig. 1(a). When the input light is coupled into the bus waveguide, the coupled evanescent-wave between the free-hanging waveguide and the bus waveguide produces an attractive gradient force. As a result, the free-hanging waveguide is driven to move freely in nanoscale displacement as shown in Figs. 1(b) and 1(c). The free-hanging waveguide used in the actuator has a

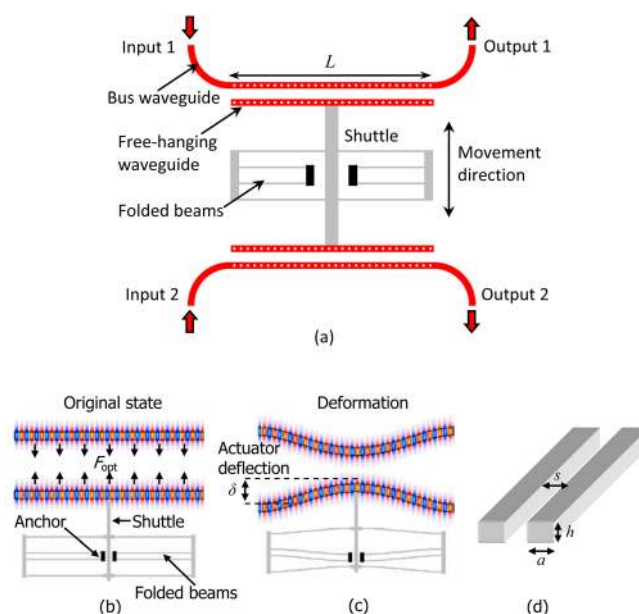


FIG. 1. (Color online) Working principle of the nano-optomechanical actuator. (a) Schematic diagram of the actuator, (b) the original state of the free-hanging waveguide, (c) the deformation state of the free-hanging waveguide, and (d) schematic of the parallel waveguides.

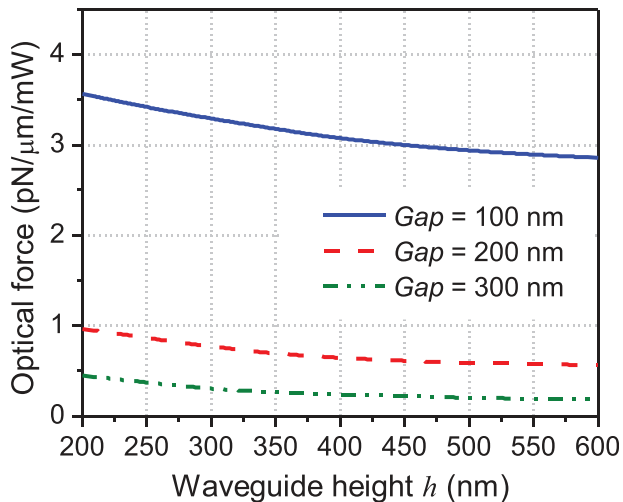
<sup>a)</sup>Author to whom correspondence should be addressed. Electronic mail: caih@ime.a-star.edu.sg.

dimension of  $310 \text{ nm} \times 220 \text{ nm}$  (width  $\times$  height) Si core (Fig. 1(d)), surrounded by a  $2 \mu\text{m}$   $\text{SiO}_2$  cladding. The free-hanging waveguide is released with a length of  $L$  (e.g.,  $L = 50 \mu\text{m}$ ), allowing it to be deformed by the optical force between the two parallel waveguides.

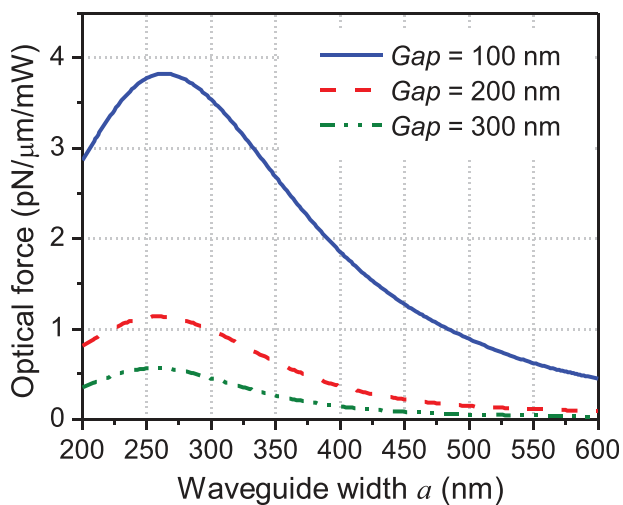
When the optical power ( $P$ ) is coupled into the parallel waveguides, the attractive gradient force ( $F_{\text{opt}}$ ) is induced and evenly distributed along the waveguide length  $L$ , which is expressed as<sup>16</sup>

$$\frac{F_{\text{opt}}}{L} = - \left. \frac{P}{v_g \omega} \frac{d\omega}{ds} \right|_k, \quad (1)$$

where  $\omega$  is the optical input frequency,  $v_g$  is the group velocity,  $k$  is the wave vector, and  $s$  is the gap between the waveguides. Equation (1) has been verified to be equivalent to the Maxwell stress tensor formalism.<sup>16</sup> It indicates that a decrease in frequency leads to a lowering of system energy, and hence induces an attractive force. In particular, a change of the waveguide separation by  $ds$  causes the energy coupled into the waveguide eigenmode to vary, resulting in the eigen-



(a)



(b)

FIG. 2. (Color online) The optical force as a function of the waveguide dimensions. (a) The waveguide height  $h$ , and (b) the waveguide width  $a$ .

mode frequency shifting by  $d\omega$ . By first order approximation,  $d\omega/ds$  is a constant for a small change of the gap width, and thus the gradient force increases linearly with the optical power. In order to enhance the optical force, holes are arranged along the waveguide to form one-dimensional photonic crystal.<sup>17</sup> Based on the simulation results, the group velocity ( $v_g$ ) in the photonic crystal waveguide can be reduced to a minimum of  $v_g/c = 0.08$  ( $c$  is the speed of light in vacuum). Therefore, the optical force is increased by six-fold from  $0.17 \text{ pN}/\mu\text{m}/\text{mW}$  to  $1.01 \text{ pN}/\mu\text{m}/\text{mW}$  (per unit length of the actuator) at the wavelength of  $1550 \text{ nm}$ .

Based on the static Euler-Bernoulli beam equation and boundary conditions, the mechanical deflection ( $\delta$ ) at any point along the suspended waveguides can be determined as

$$\delta = - \frac{F_{\text{opt}}}{24EIL} (x^4 - 2Lx^3 + L^2x^2), \quad (2)$$

where  $E$  is the waveguide's Young's modulus,  $I$  is its moment of inertia, and  $x$  is the position along the suspended waveguide length ( $0 \leq x \leq L$ ). It is noted that the maximum deflection occurs at  $x = L/2$ . By combining Eqs. (1) and (2) and substituting  $I = ha^3/12$  (here  $h$  and  $a$  are the waveguide height and width, respectively), the maximum deflection is derived as

$$\delta_{\text{max}} = - \frac{PL^4}{32Eha^3v_g\omega} \left. \frac{d\omega}{ds} \right|_k. \quad (3)$$

Therefore, the displacement  $D$  of the nanoscale actuator can be obtained with  $D = \delta_{\text{max}}$ . Equation (3) provides the insight for the physical design criteria of the nanoscale actuator. The displacement  $D$  varies linearly with optical power  $P$ , which allows precise optical control of the actuator displacement by varying the input optical power. Meanwhile,  $D$  is also dependent on the dimension of the waveguide (free-hanging length ( $L$ ), height ( $h$ ), and width ( $a$ )). A maximum displacement of  $40.8 \text{ nm}$  is achieved with a free-hanging waveguide of  $60 \mu\text{m} \times 310 \text{ nm} \times 220 \text{ nm}$  ( $L \times a \times h$ ), which is much smaller than the typically displacement of MEMS actuator driven by the electrostatic force (typically  $45\text{-}\mu\text{m}$ ).<sup>2</sup> The nanoscale opto-mechanical actuator provides nanoscale resolution at high precision, which is critical and sufficient to control and manipulate light. However, it is noted that

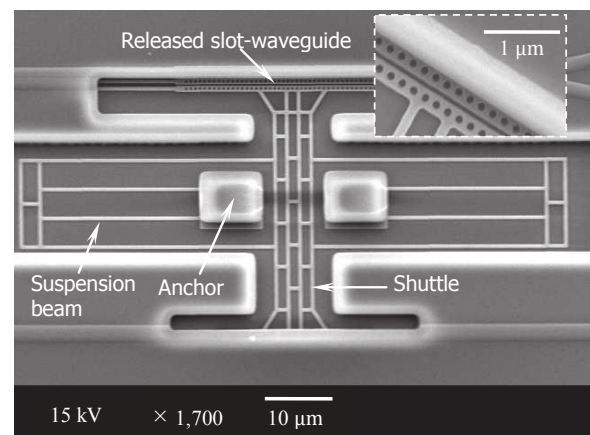


FIG. 3. Scanning electron micrograph of the actuator and the waveguides. Inset: close-up to the released slot-waveguide.

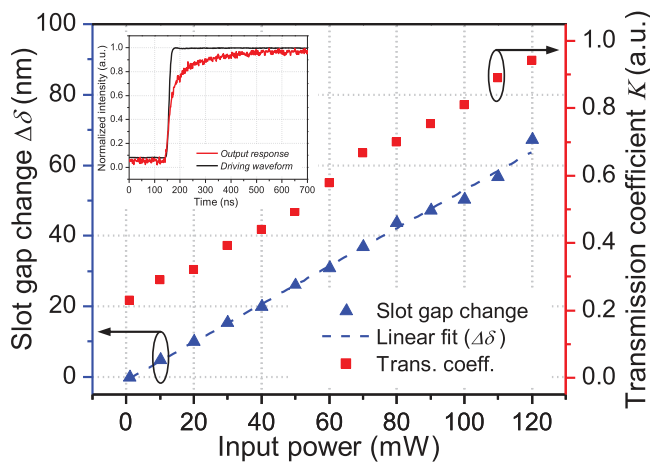


FIG. 4. (Color online) Measured displacement of the nano-optomechanical actuator versus the input optical power. The transmission coefficient is also plotted. Inset: dynamic response of the actuator under a 8-MHz modulated light signal.

changing the waveguide cross-section affects the waveguide dispersion (i.e.,  $d\omega/ds$ ) as well, which will be further discussed.

The dispersion relationship of the waveguide is obtained from numerical simulations. Fig. 2 plots the optical forces as the function of the waveguide cross-sectional dimensions under different gaps ( $s$ ). It can be concluded that larger optical force is achieved at narrower gap. The effect of waveguide height on the optical force (Fig. 2(a)) is limited and insignificant as compared with the waveguide width (Fig. 2(b)). The optical force exhibits a maximum at  $a = 260$  nm and decreases as  $a$  increases. This is because the evanescent coupling of the guided light produces the largest gradient of optical distribution at a specific size of the waveguide cross-section. Although simulations suggest that a smaller waveguide cross-section is preferable to produce larger optical forces, it should be noted that the optical loss also increase significantly with smaller waveguide cross-section. From fabrication point of view, the lithography techniques and the wafer thickness also impose limitations for the practical dimensions of waveguide fabrication.

The nanoscale opto-mechanical actuator was designed and fabricated on standard silicon-on-insulator (SOI) wafer using nanosilicon photonic fabrication processes, with a silicon structure layer of 220 nm thick and 2  $\mu$ m buried oxide layer. Except for the waveguides, the shuttles and the suspension beams of the nanoscale opto-mechanical actuator, other waveguides were covered with 2  $\mu$ m thickness of SiO<sub>2</sub> cladding layer. The waveguides and other structures were patterned by deep UV lithography, followed by plasma dry etching to transfer the photo resist pattern into the substrate. After deposition and patterning the upper SiO<sub>2</sub> layer, the areas directly above the suspended features were etched away through dry etching. Finally, a buffered oxide etching solution selectively undercut the buried oxide layer so as to release the parts of movable structures and the waveguides. The scanning electron microscope (SEM) images of the fabricated nano-optomechanical actuators and free-hanging waveguide are shown in Fig. 3, and a close-up to the free-hanging waveguide

is shown in Fig. 3. The free-hanging waveguide has a dimension of 50  $\mu$ m  $\times$  310 nm  $\times$  220 nm (length  $\times$  width  $\times$  height). The initial gap of the parallel waveguide is 200 nm, which can be tuned by varying the input optical power.

Figure 4 plots the characterized relationship between the gap variation and the input power with light wavelength of 1556 nm. A linear relationship is obtained with a gradient of 0.558 nm/mW. It is noted that the change of the gap will affect the optical coupling of the waveguides and thus the transmission coefficient.<sup>18</sup> Therefore, the gap variation ( $\Delta\delta$ ) can be characterized by the transmission  $K$  of the optical power, where  $K = f(a)\exp[-\gamma(s + \delta - a)]$  (see Ref. 18). In the experiment, the maximum gap variation achieved is 67 nm in which the transmission coefficient increases from 0.21 to 0.93 due to the reduction of the gap. The dynamic response of the actuator is modulated by light signal (8 MHz, 10 mW power) as shown in Fig. 4. The output power is normalized with respect to the maximum output power. The response time is measured as 94.5 ns, which corresponds to the optical signal variation from 10% to 90% of the steady state optical power level. Compared with traditional MEMS actuators driven by electrostatic force, the response time is reduced from milliseconds to nanoseconds.

In conclusion, a nanoscale opto-mechanical actuator driven by the gradient optical force has been designed, fabricated, and demonstrated. The maximum achieved displacement is 67 nm with a response time of 94.5 ns. The nanoscale optomechanical actuator can provide optical driven force of 1.01 pN/ $\mu$ m/mW. Comparing with the electrostatic driven MEMS actuators, the advantages are not only with high resolution of nanometer-scale displacement but also fast response at the nanosecond level. It has high potential in a wide range of applications, including optical signal processing, chemical, and biological sensing.

- <sup>1</sup>J. D. Grade, H. Jerman, and T. W. Kenny, *J. Microelectromech. Syst.* **12**, 335 (2003).
- <sup>2</sup>J. Li, Q. X. Zhang, and A. Q. Liu, *Sens. Actuators, A* **102**, 286 (2003).
- <sup>3</sup>M. Wu, O. Solgaard, and J. Ford, *J. Lightwave Technol.* **24**, 4433 (2006).
- <sup>4</sup>A. Q. Liu and X. M. Zhang, *J. Micromech. Microeng.* **17**, R1 (2007).
- <sup>5</sup>S. Krylov and Y. Bernstein, *Sens. Actuators, A* **130–131**, 497 (2006).
- <sup>6</sup>M. C. Oh, J. W. Kim, K. J. Kim, and S. S. Lee, *IEEE Photon Technol. Lett.* **21**, 501 (2009).
- <sup>7</sup>R. Legtenberg, A. W. Groeneveld, and M. Elwenspoek, *J. Micromech. Microeng.* **6**, 320 (1996).
- <sup>8</sup>A. Ashkin, *Phys. Rev. Lett.* **24**, 156 (1970).
- <sup>9</sup>S. Chu, *Science* **253**, 861 (1991).
- <sup>10</sup>A. H. J. Yang, S. D. Moore, B. S. Schmidt, M. Klug, M. Lipson, and D. Erickson, *Nature* **457**, 71 (2009).
- <sup>11</sup>M. Eichenfield, R. Camacho, J. Chan, K. J. Vahala, and O. Painter, *Nature* **459**, 550 (2009).
- <sup>12</sup>G. S. Wiederhecker, L. Chen, A. Gondarenko, and M. Lipson, *Nature* **462**, 633 (2009).
- <sup>13</sup>D. Van Thourhout and J. Roels, *Nature Photon.* **4**, 211 (2010).
- <sup>14</sup>T. J. Kippenberg and K. J. Vahala, *Science* **321**, 1172 (2008).
- <sup>15</sup>M. Li, W. H. P. Pernice, C. Xiong, T. Baehr-Jones, M. Hochberg, and H. X. Tang, *Nature* **456**, 480 (2008).
- <sup>16</sup>M. L. Povinelli, M. Loncar, M. Ibanescu, E. J. Smythe, S. G. Johnson, F. Capasso, and J. D. Joannopoulos, *Opt. Lett.* **30**, 3042 (2005).
- <sup>17</sup>M. L. Povinelli, M. Ibanescu, S. G. Johnson, and J. D. Joannopoulos, *Appl. Phys. Lett.* **85**, 1466 (2004).
- <sup>18</sup>K. Okamoto, *Fundamentals of Optical Waveguides*, 2nd ed. (Elsevier, Boston, 2006).